Supporting Information

Highly Active and Durable Iron-Cobalt Alloy Catalyst Encapsulated in N-doped Graphitic Carbon Nanotubes for Oxygen Reduction Reaction by Nanofibrous Dicyandiamine Template

Li An, [a] *Ning Jiang,* [b] *Biao Li,* [b] *Shixin Hua,* [a] *Yutong Fu,* [a] *Jiaxi Liu,* [a] *Wei Hao,* [a] *Dingguo Xia*[*,b] *Zaicheng Sun*[*a]

[a]Beijing Key Laboratory of Green Catalysis and Separation, College of Environmental and Energy Engineering, Beijing University of Technology, Beijing 100124, People's Republic of China

[b] Beijing Key Laboratory of Theory and Technology for Advanced Batteries Materials, College of Engineering, Peking University, Beijing 100871, People's Republic of China

KEYWORDS: FeCo@N-GCNT-FD, FeCo@N-GCNT, oxygen reduction reaction, electrocatalyst

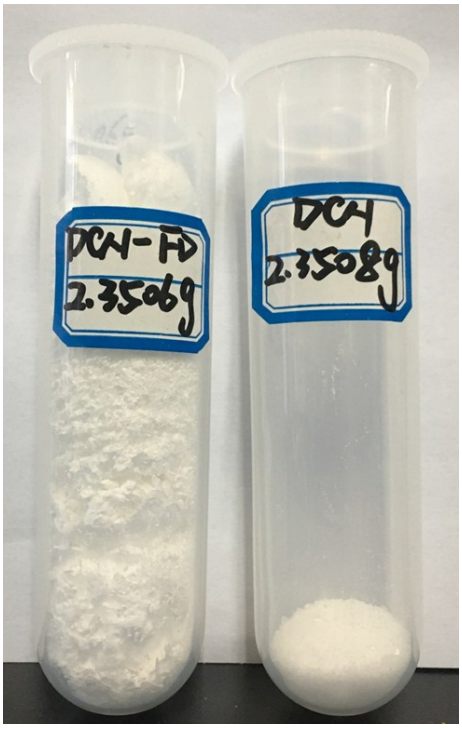

Figure S1. Photographs of the freeze-drying dicyandiamide (left) and pristine dicyandiamide (right)

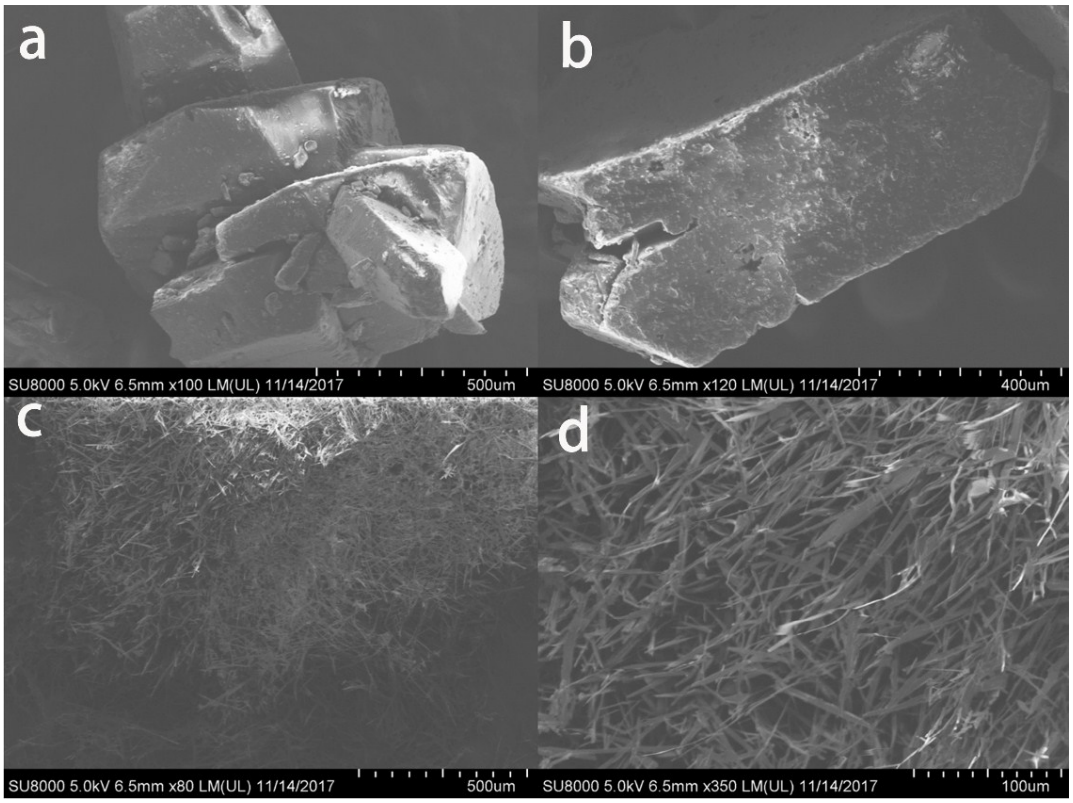

Figure S2. SEM image of the (a, b) pristine and (c, d) freeze-drying dicyandiamide.

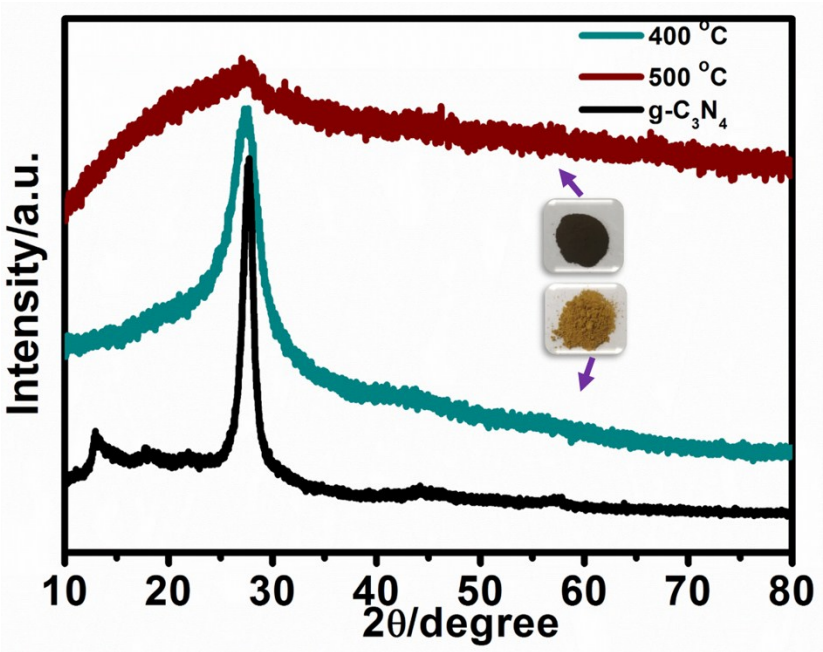

Figure S3. Powder XRD patterns of g-C_3N_4 and FeCo@NGCNT-FD annealed at 400, 500 °C under Ar atmosphere after acid etching.

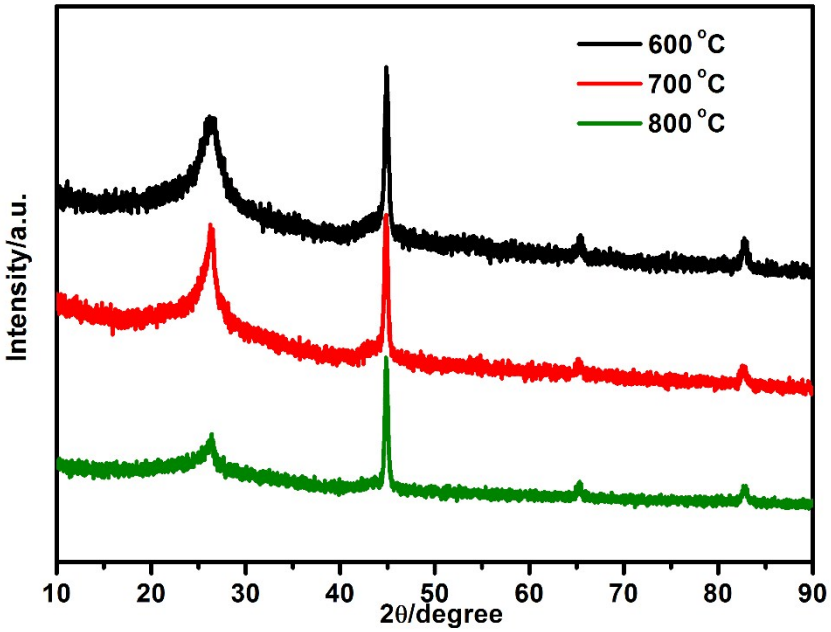

Figure S4. Powder XRD patterns of (a) FeCo@NGCNT-FD annealed at 600~800 °C and (b) FeCo@NGCNT annealed at 800 °C under Ar atmosphere after acid etching.

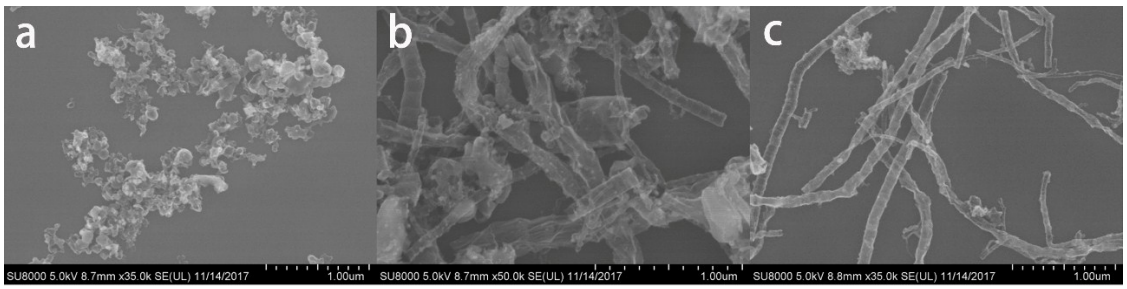

Figure S5. Typical SEM images of (a) FeCo@N-GCNT-FD-600 °C, (b) FeCo@N-GCNT-FD-700 °C and (c) FeCo@N-GCNT-FD-800 °C.

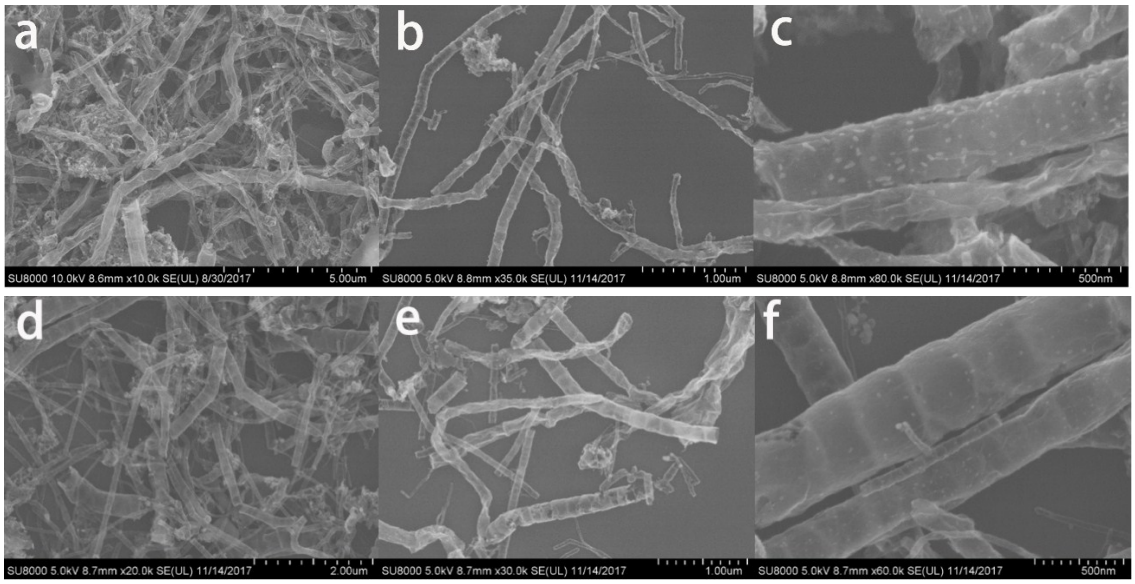

Figure S6. Typical SEM different magnification images of (a~c) FeCo@N-GCNT-FD, (d~f) FeCo@N-GCNT.

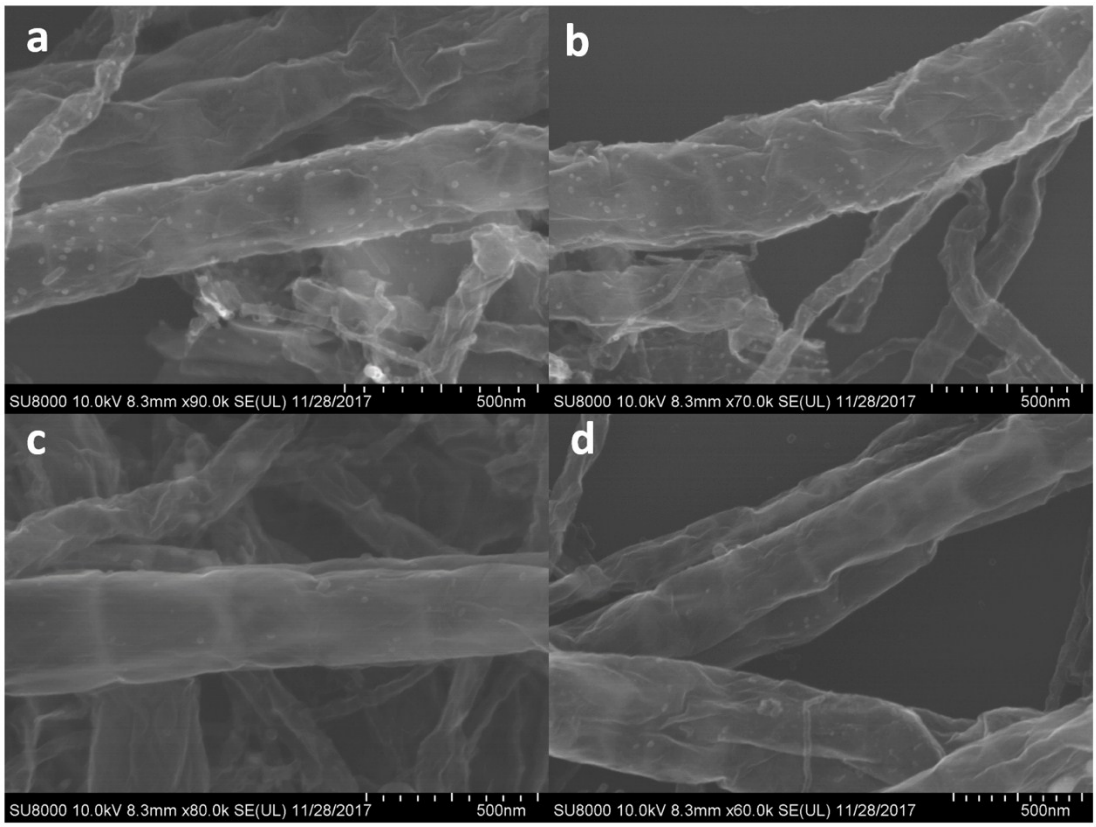

Figure S7. Typical SEM images of (a, b) FeCo@N-GCNT-FD and (c, d) FeCo@N-GCNT, respectively.

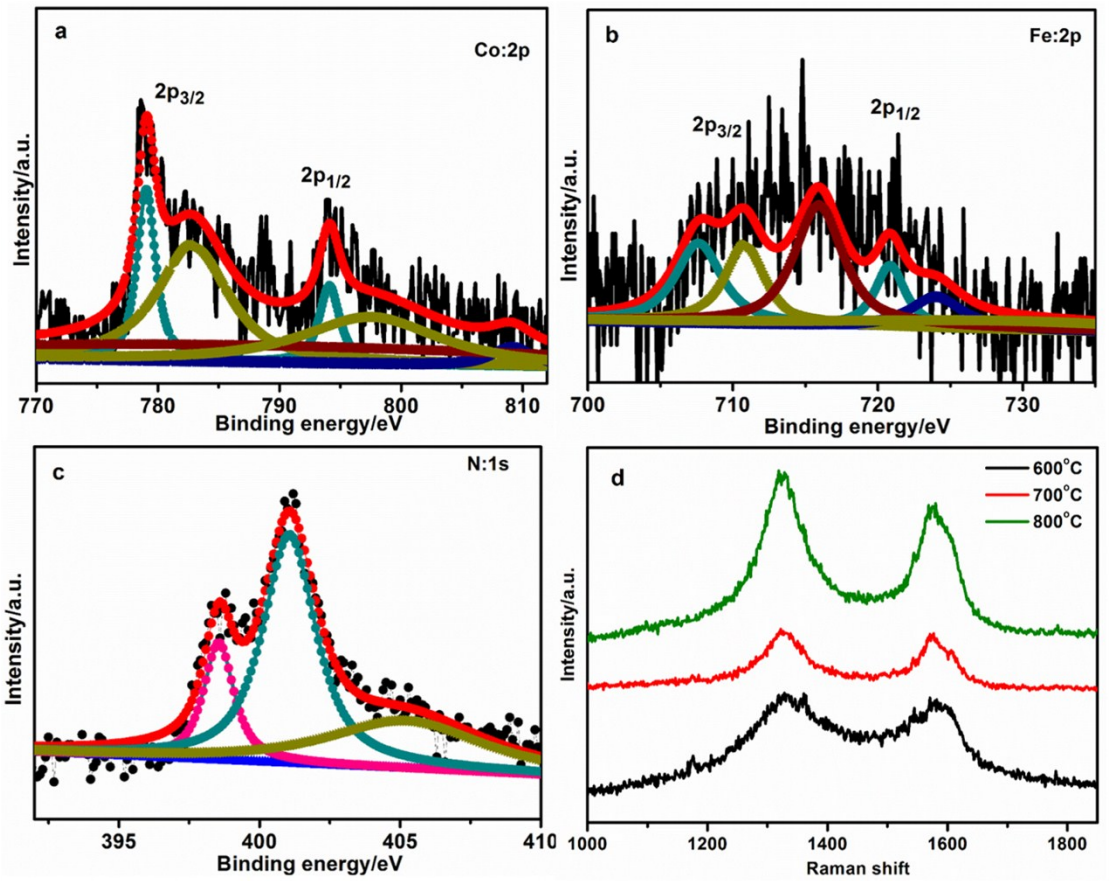

Figure S8. High-resolution XPS spectra of a) Co 2p, b) Fe 2p and c) N 1s core levels in FeCo@N-GCNT; (d) Raman spectrum of FeCo@N-GCNT annealed at 600-800 ^{o}C.

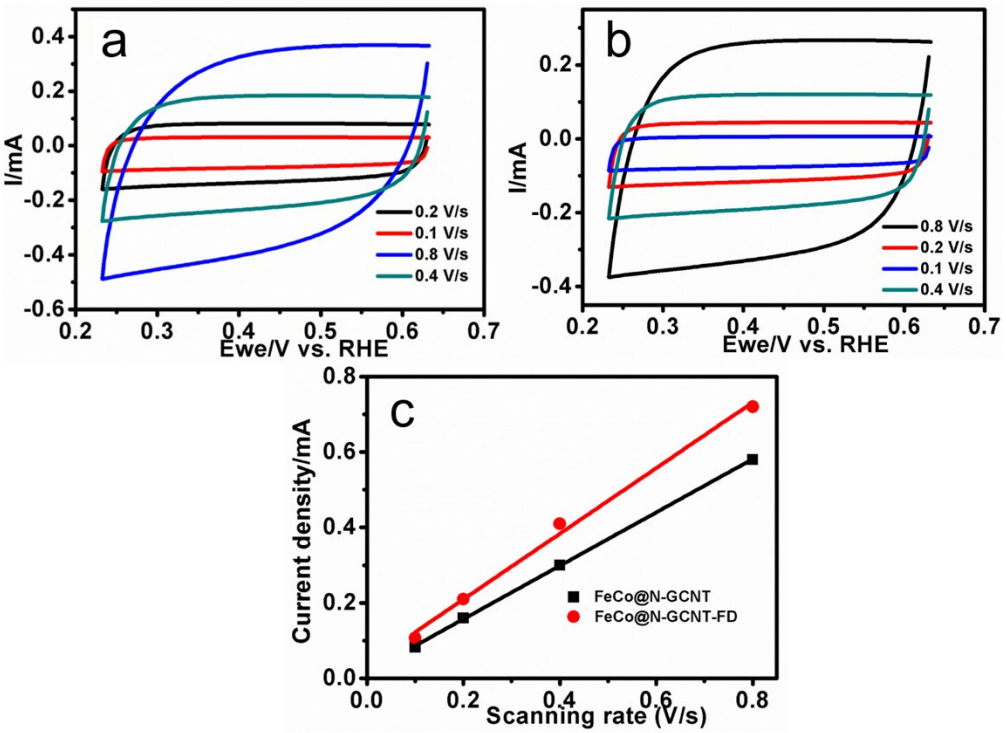

Figure S9. (a, b) CV curves of FeCo@N-GCNT and FeCo@N-GCNT-FD with different scan rates in 0.1 M KOH solution; (c) Charging current density differences (Δj) plotted against scanning rates. Δj is the difference between anodic and cathodic current at the potential of 0.45 V, where no redox current peaks are observed.

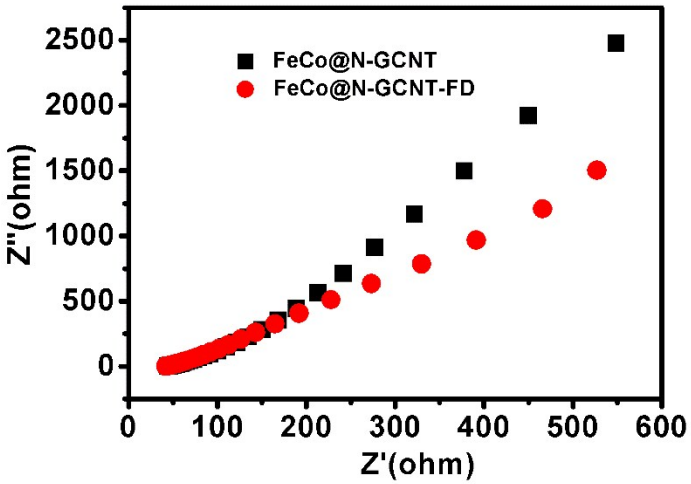

Figure S10. Nyquist plots of FeCo@N-GCNT and FeCo@N-GCNT-FD at 0.75 V vs RHE of 5 mV in the frequency range from 0.01 Hz to 100 kHz.

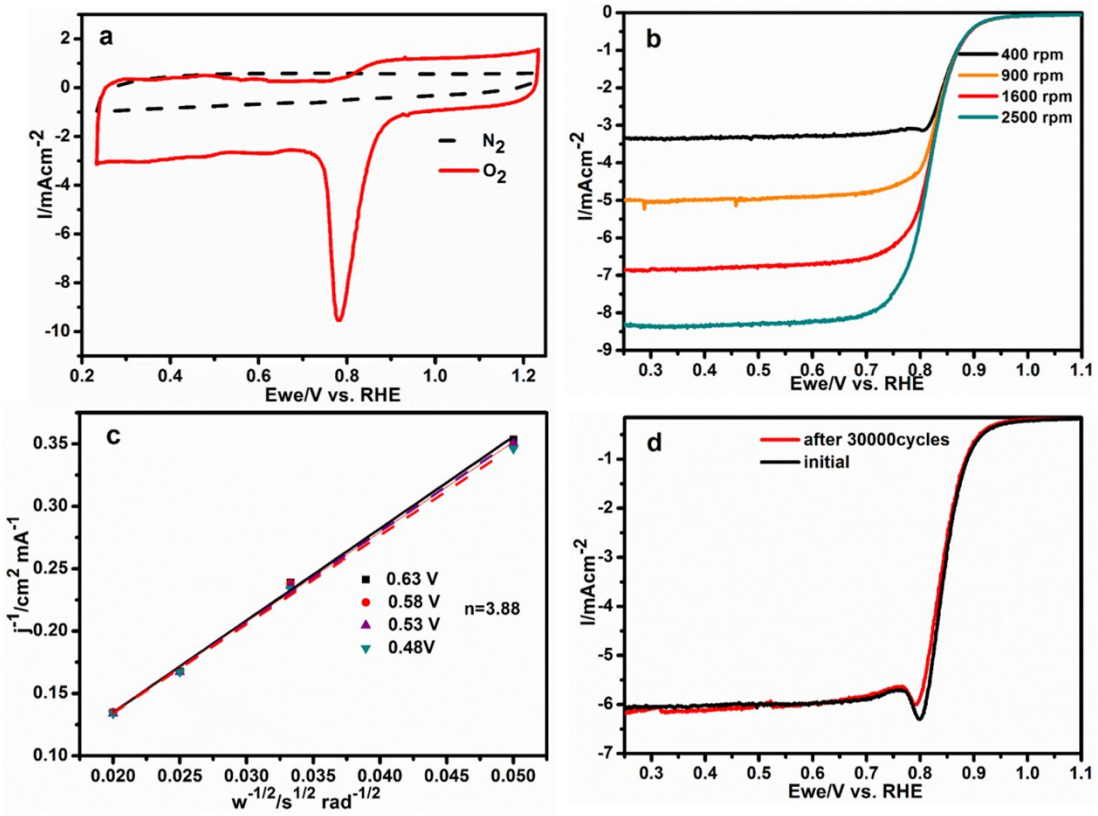

Figure S11. (a) CV curves of FeCo@N-GCNT-FD catalyst at a scan rate of 50 mV s^{-1} in N_2 or O_2-saturated 0.1 M KOH solution. (b) RDE voltammetric response for the ORR in O_2-saturated 0.1M KOH at a scan rate of 10 mV s^{-1} at different rotation rate. (c) K-L plots for FeCo@N-GCNT-FD catalyst at different potentials. (d) RDE polarization curves of the FeCo@N-GCNT-FD electrocatalyst before and after 30,000 cycles in O_2-saturated 0.1 M KOH. Potential cycling was carried out between 0.6 and 1.2 V *vs* RHE at 200 mV s^{-1}.

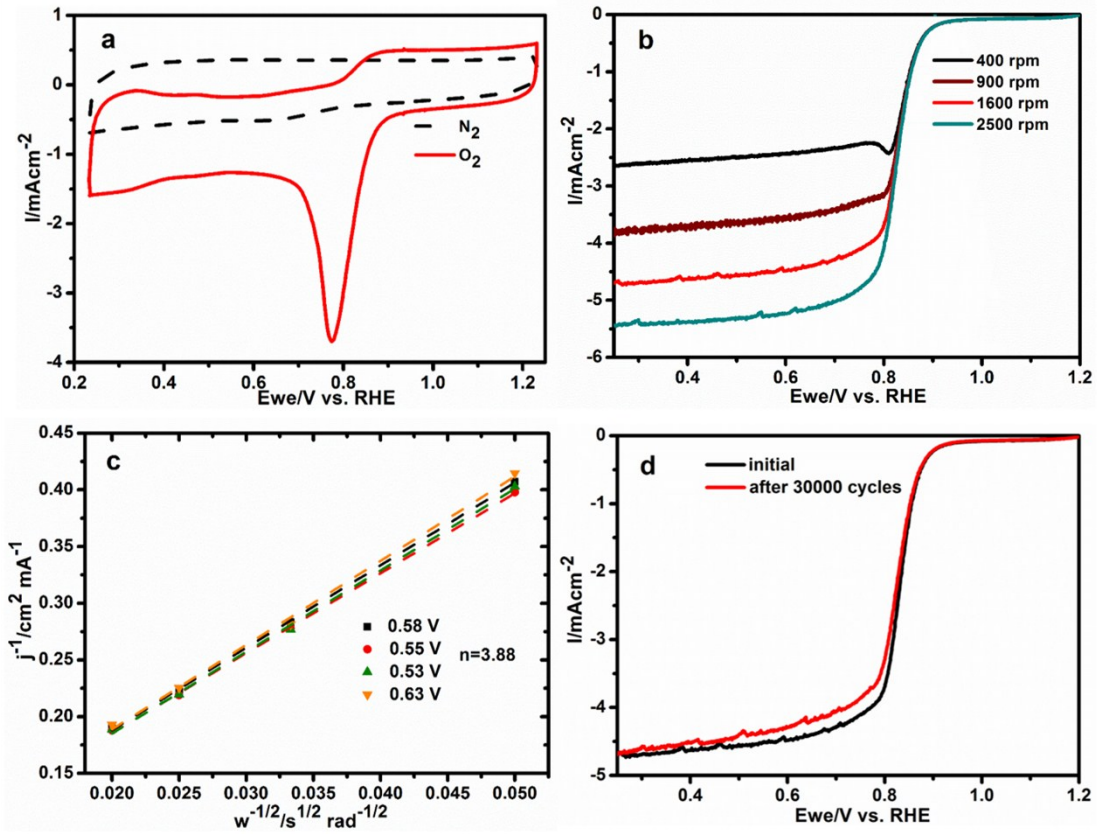

Figure S12. (a) CV curves of FeCo@N-GCNT catalyst at a scan rate of 50 mV s^{-1} in N_2 or O_2-saturated 0.1 M KOH solution. (b) RDE voltammetric response for the ORR in O_2-saturated 0.1M KOH at a scan rate of 10 mV s^{-1} at different rotation rate. (c) K-L plots for FeCo@N-GCNT catalyst at different potentials. (d) RDE polarization curves of the FeCo@N-GCNT electrocatalyst before and after 30,000 cycles in O_2-saturated 0.1 M KOH. Potential cycling was carried out between 0.6 and 1.2 V *vs* RHE at 200 mV s^{-1}.

Table S1. ORR activities of the non-precious electrocatalysts in alkaline medium.

Catalyst	Onset potential (V) vs RHE	Half potential (V) vs RHE	Kinetic activity (i_k) (0.7 V)	Reference
$Co_xMn_{3-x}O_4$	0.87	N. A	N. A	S1
Co_3O_4/N-Graphene	0.90	0.83	i_k=52.6 mA cm^{-2}	S2
G–Co/CoO	N. A	0.79	N. A	S3
$Co_{1-x}S$/RGO	0.87	0.78	i_k=3.8 mA cm^{-2}	S4
$CoSe_2$/C	0.85	0.71	N. A	S5
$Co_{1.67}Te_2$/C	0.79	0.62	N. A	S6
Ag-Co	0.90	N. A	N. A	S7
MnO/m-N-C	0.90	0.81	N. A	S8
N-Fe-CNT/CNP	N. A	0.93	N. A	S9
Co@CoO_x/NCNT	0.94	0.80	i_k=92.6 mA cm^{-2}	S10
Fe−N-Doped CC	0.94	0.83	N. A	S11
CuCo@NC	0.96	0.88	N. A	S12
Fe/Fe_3C@C	0.91	0.83	N. A	S13
Fe_3C@N-CNT	0.97	0.85	N. A	S14
GL-Fe/Fe_5C_2/NG-800	0.98	0.86	N. A	S15
Fe/Co-NpGr	0.93			S16
FeCo@N-GCNT	0.91	0.83	i_k=84.5 mA cm^{-2}	This work
FeCo@N-GCNT-FD	0.96	0.88	i_k=284.7 mA cm^{-2}	This work

N.A.: Not available

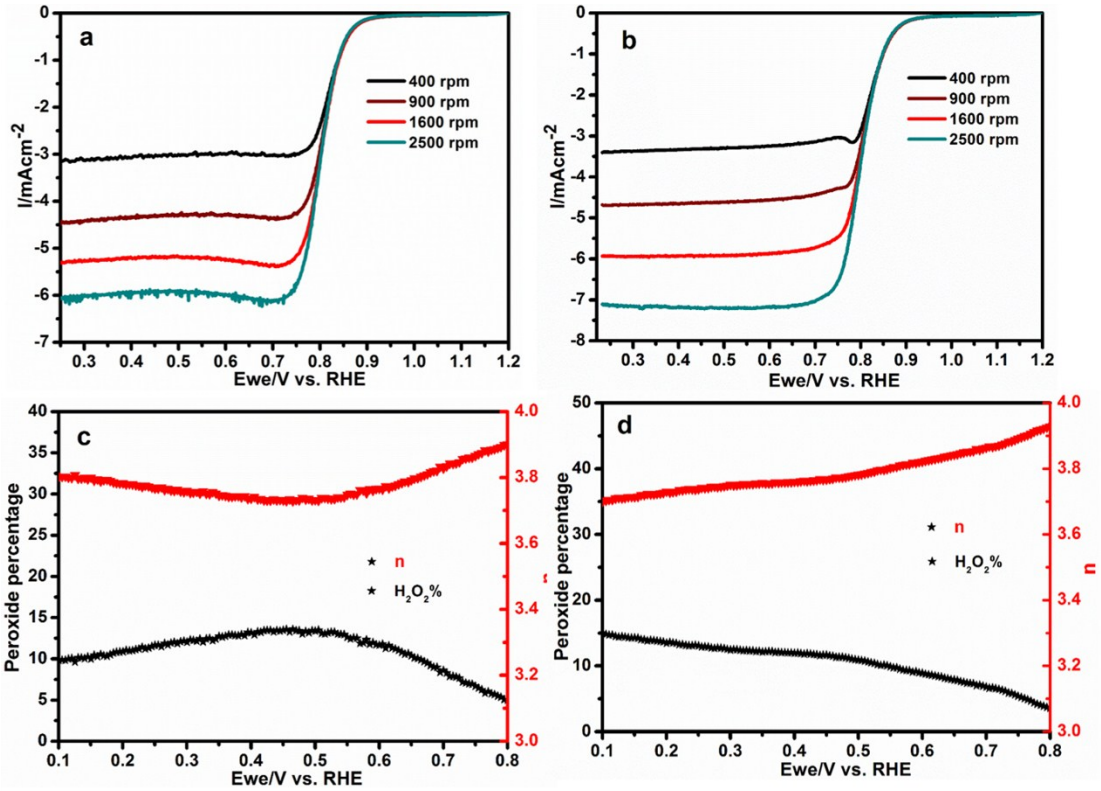

Figure S13. (a, b) RDE voltammetric response of FeCo@N-GCNT-FD-600 ^{o}C and 700 ^{o}C for the ORR in O_2-saturated 0.1M KOH at a scan rate of 10 mV s^{-1} at different rotation rate, respectively. (c, d) Peroxide percentage and electron transfer number (n) of FeCo@N-GCNT-FD-600 ^{o}C and FeCo@N-GCNT-FD-700 ^{o}C within the potential range of 0.1 V to 0.8 V, respectively.

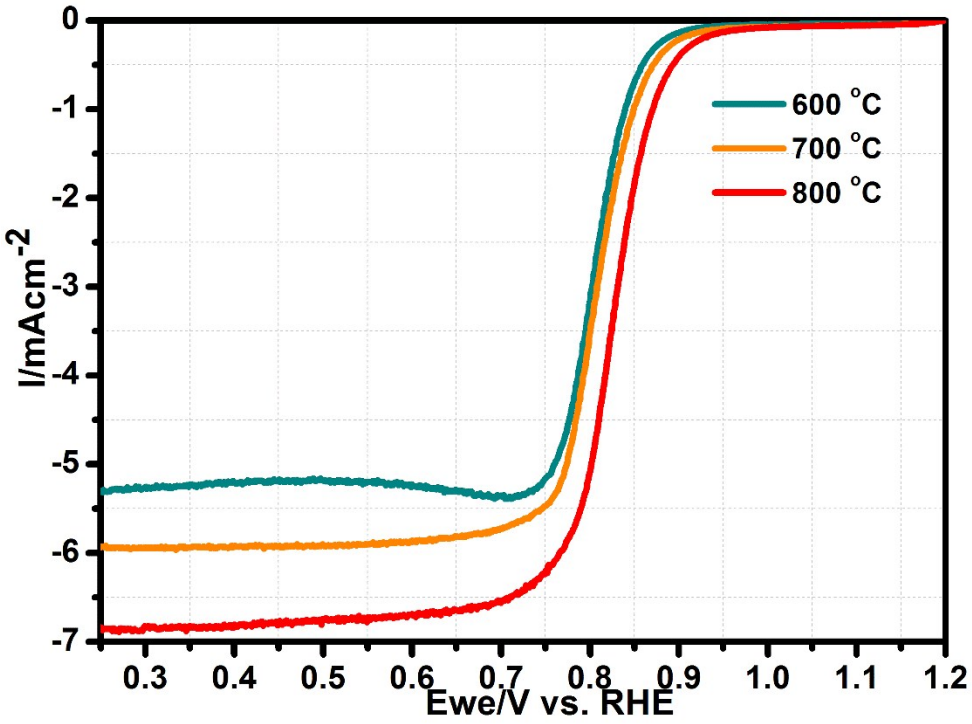

Figure S14. Comparison of the RDE polarization curves of the FeCo@N-GCNT-FD annealed at 600~800 °C electrocatalysts in O_2-saturated 0.1 M KOH at 1600rpm.

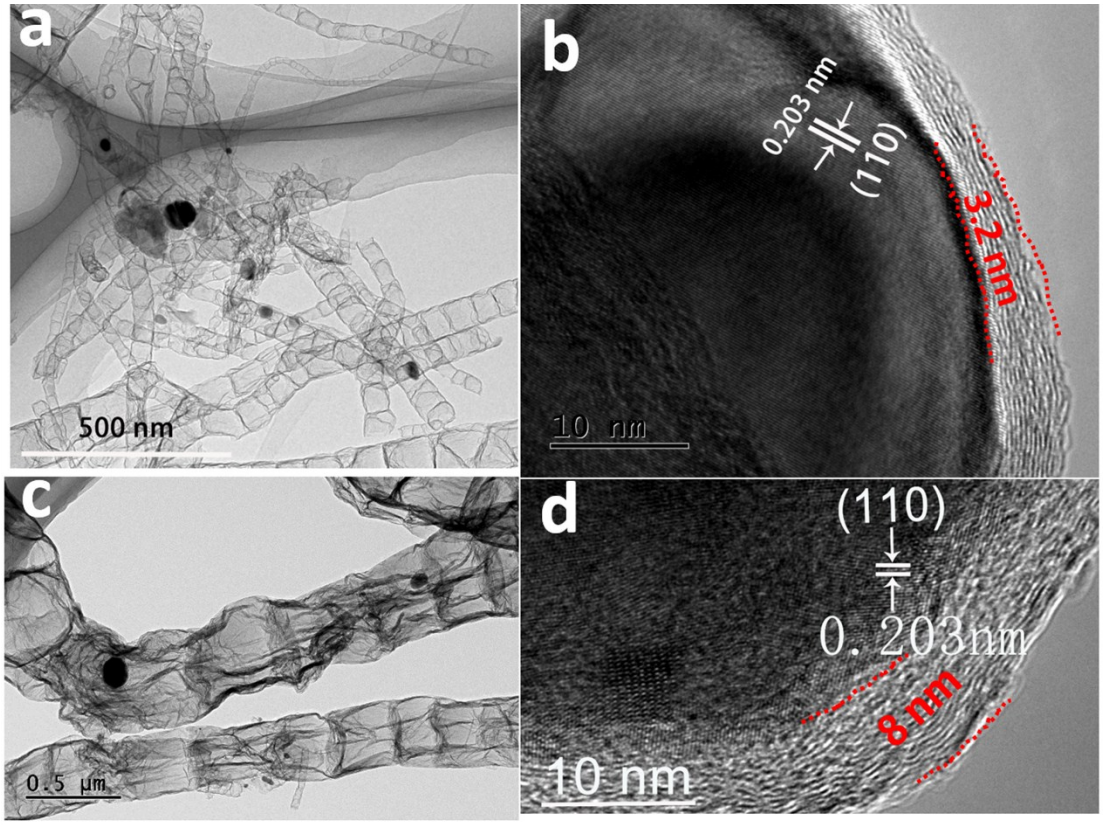

Figure S15. a, c) TEM and b, d) HRTEM images of FeCo@N-GCNT-FD and FeCo@N-GCNT after ADT test, respectively.

Table S2. ORR activities of the non-precious electrocatalysts in acid medium.

Reference	Catalyst	Onset Potential (V) vs. RHE	Half-wave Potential (V) vs. RHE	Medium
J. Am. Chem. Soc. 2015, 137, 5414−5420	CPANI-Fe	above 0.8	0.75	0.1 M $HClO_4$
J. Am. Chem. Soc., 2014, 136, 11027−11033	Fe-N-C	0.9	0.65	0.1 M $HClO_4$
Electrochim. Acta, 2008, 53, 7703−7710	Carbon supported Fe-N catalysts	0.88	0.62	0.1 M H_2SO_4
Angew. Chem. Int. Ed., 2013, 52, 10753 –10757	$Co_xMo_{1-x}O_yN_z/C$	0.654	0.45	0.1 M $HClO_4$
ACS Catal. 2015, 5, 1857−1862	$Co_{0.50}Mo_{0.50}N_y$/NCNCs	0.808	0.6	0.5 M H_2SO_4
Angew. Chem. Int. Ed. 2011, 50, 10969 –10972	$Co_{1-x}S$/RGO	0.8	-	0.5 M H_2SO_4
Chem. Mater. 2015, 27, 544−549	CoNPs@NG	0.82	0.7	0.5 M $HClO_4$
J. Am. Chem. Soc. 2015, 137, 3165−3168	Fe-P-900	0.84	0.6	0.1 M $HClO_4$
Adv. Mater. 2015, 27, 3431−3436	PCN-FeCo/C	0.90	0.73	0.1 M $HClO_4$
J. Am. Chem. Soc., 2015, 137, 1436−1439	PMF-800	0.886	0.62	0.1 M $HClO_4$
J. Am. Chem. Soc., 2017, 139, 14143–14149	atomic Fe PGM-free	0.97	0.85	0.1 M $HClO_4$
ACS Catal. 2017, 7, 6864−6871	Co−N/CNFs	0.82	0.70	0.1 M $HClO_4$
This work	FeCo@N-GCNT-FD	0.82	0.65	0.5 M H_2SO_4

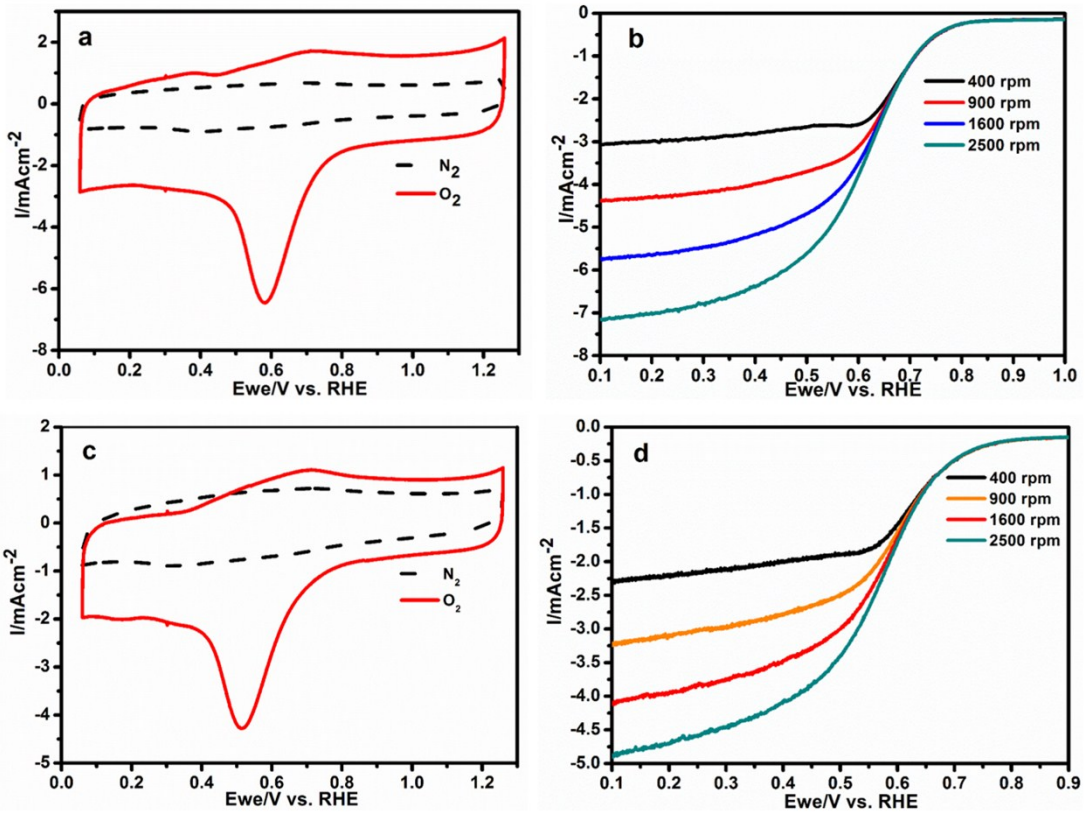

Figure S16. (a, c) CV curves of FeCo@N-GCNT-FD and FeCo@N-GCNT catalysts at a scan rate of 50 mV s^{-1} in N_2 or O_2-saturated 0.5 M H_2SO_4 solution. (b, d) RDE voltammetric response for the ORR in O_2-saturated 0.5 M H_2SO_4 at a scan rate of 10 mV s^{-1} at different rotation rates.

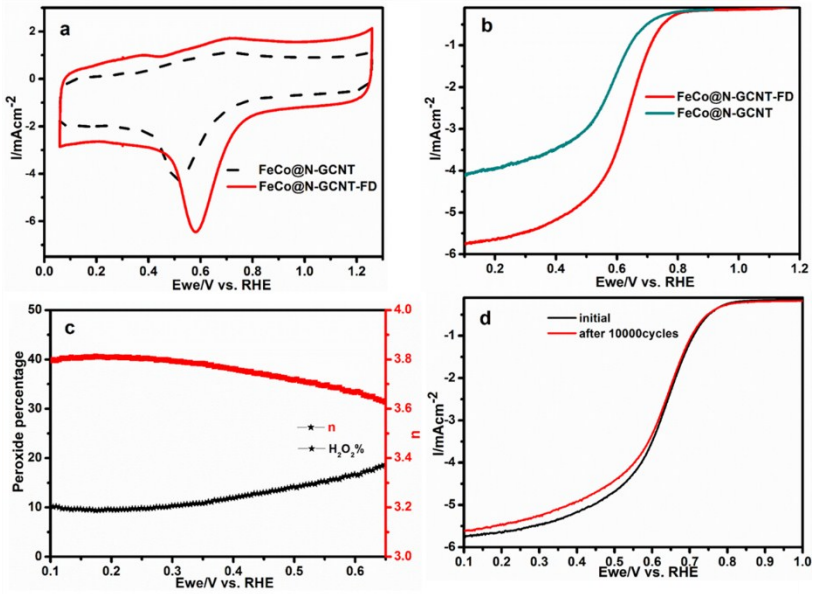

Figure S17. (a) CV curves of FeCo@N-GCNT-FD and FeCo@N-GCNT catalysts at a scan rate of 50 mV s^{-1} in N_2 or O_2-saturated 0.5 M H_2SO_4 solution. (b) LSV curves for different samples in O_2-saturated 0.5 M H_2SO_4 solution at a rotation rate of 1600 rpm. (c) Peroxide percentage and electron transfer number (n) of FeCo@N-GCNT-FD within the potential range of 0.1 V to 0.7 V. (d) RDE polarization curves of the FeCo@N-GCNT-FD electrocatalyst before and after10,000 cycles in O_2-saturated 0.5 M H_2SO_4. Potential cycling was carried out between 0.6 and 1.2 V *vs* RHE at 200 mV s^{-1}.

References

S1. F. Cheng, J. Shen, B. Peng, Y. Pan, Z. Tao, J. Chen, Nat. Chem. 3 (2011) 79.

S2. Y. Liang, Y. Li, H. Wang, J. Zhou, J. Wang, T. Regier, H. Dai, Nat. Mater. 10 (2011) 780.

S3. S. Guo, S. Zhang, L. Wu, S. Sun, Angew. Chem. Int. Ed. 124 (2012) 11940.

S4. H. Wang, Y. Liang, Y. Li, H. Dai, Angew. Chem. Int. Ed. 50 (2011) 10969.

S5. Y. Feng, N. Alonso-Vante, Electrochimi. Acta 72 (2012) 129.

S6. G. Wu, G. Cui, D. Li, P. K. Shen, N. Li, J. Mater. Chem. 19 (2009) 6581.

S7. A. Holewinski, J. C. Idrobo, S. Linic, Nat. Chem. 4 (2014) 828.

S8. Y. Tan, C. Xu, G. Chen, X. Fang, N. Zheng, Q. Xie, Adv. Fun. Mater. 22 (2012) 4584.

S9. H. T. Chung, J. H. Won, P. Zelenay, Nature Commun. 4, (2013) 1922.

S10. C. Lin, S. S. Shinde, Z. Jiang, X. Song, Y. Sun, L. Guo, H. Zhang, J. -Y. Jung, X. Li, J. H. Lee, J Mater. Chem. A 2017, 5, 13994.

S11. G. A. Ferrero, K. Preuss, A. Marinovic, A. B. Jorge, N. Mansor, D. J. L. Brett, A. B. Fuertes, M. Sevilla,* M. M. Titirici*. ACS Nano 2016, 10, 5922−5932.

S12. M. Kuang, Q. Wang, P. Han, G. Zheng. Adv. Energy Mater. 2017, 1700193.

S13. Y. Hou, T. Huang, Z. Wen, S. Mao, S. Cui, J. Chen. Adv. Energy Mater. 2014, 4, 1400337

S14. B. Y. Guan, L. Yua, X. W. (David) Lou. Energy Environ. Sci. 2016, 9, 3092−3096.

S15. E. Hu, X. Y. Yu, F. Chen, Y. Wu, Y. Hu*, X. W. (David) Lou*. Adv. Energy Mater. 2017, 1702476

S16. T. Palaniselvam, V. Kashyap, S. N. Bhange, J. B. Baek*, S. Kurungot *. Adv. Funct. Mater. 2016, 26, 2150–2162.